Published in final edited form as:
Nano Lett. 2010 February 10; 10(2): 547. doi:10.1021/nl9034219.

Subthreshold Regime has the Optimal Sensitivity for Nanowire FET Biosensors

Xuan P. A. Gao[*,†], **Gengfeng Zheng**[*,‡], and **Charles M. Lieber**[§,‖]

[†]Department of Physics, Case Western Reserve University, Cleveland, OH 44106, USA

[‡]Laboratory of Advanced Materials, Fudan University, Shanghai, 200433, P. R. China

[§]Department of Chemistry and Chemical Biology, Harvard University, Cambridge, MA 02138, USA

[‖]Division of Engineering and Applied Science, Harvard University, Cambridge, MA 02138, USA

Abstract

Nanowire field-effect transistors (NW-FETs) are emerging as powerful sensors for detection of chemical/biological species with various attractive features including high sensitivity and direct electrical readout. Yet to date there have been limited systematic studies addressing how the fundamental factors of devices affect their sensitivity. Here we demonstrate that the sensitivity of NW-FET sensors can be exponentially enhanced in the subthreshold regime where the gating effect of molecules bound on surface is the most effective due to the reduced screening of carriers in NWs. This principle is exemplified in both pH and protein sensing experiments where the operational mode of NW-FET biosensors was tuned by electrolyte gating. The lowest charge detectable by NW-FET sensors working under different operational modes is also estimated. Our work shows that optimization of NW-FET structure and operating conditions can provide significant enhancement and fundamental understanding for the sensitivity limits of NW-FET sensors.

Due to their comparable sizes to biomolecules, sensors based on nanomaterials (e.g. nanowires,[1-8] nanotubes,[9-11] and nanoparticles[12,13]) have great potential in sensitive biological detections. Several studies based on device properties and kinetic responses of the nanomaterial sensors have been reported recently.[14,15] For NW biosensors operated as FETs,[1] the sensing mechanism is the field gating effect of charged molecules on the carrier conduction inside NW. Compared to devices made of micro- or bulk materials, the much better sensitivity of nano-devices is closely related to the reduced dimensionality and larger surface/volume ratio. Therefore it is natural to expect that the highest sensitivity should be achieved when the whole volume of nano-device is gated by surface charges. This scenario can be realized when the carrier screening length is much larger than the radius of NW, *R*. Without losing generality, we discuss the screening controlled sensing sensitivity using boron-doped silicon NWs (p-type SiNWs) as an example. Previously, the conductance change of SiNW FETs was used to detect pH,[2] proteins,[2-5] DNAs,[6-8] and viruses.[16] In those studies, FET devices were operating with typical carrier concentration on the order of 10^{18}-10^{19}/cm^3 from doping in as-grown NWs (with stoichiometric ratio of a few thousands to one between silicon and dopant atoms). For hole density $p \sim 10^{18}$-10^{19}/cm^3, the screening length in silicon, λ_{Si}, is ~ 1-2 nm.[17] Therefore, charged molecules bound on surface can only gate NW within a surface layer of thickness ~ 1-2 nm. Yet typical SiNWs used for sensor application have *R* on the order of 10 nm. Only at

* To whom correspondence should be addressed. xuan.gao@case.edu; gfzheng2000@gmail.com.

Supporting Information Available. The contents of Supporting Information may include the following: This material is available free of charge via the Internet at http://pubs.acs.org.

much lower p, one has $\lambda_{Si} \gg R$ and the whole volume of NW is gated by molecules at surface. A schematic comparison between these two scenarios is shown in Figure 1 together with the screening length in silicon plotted as a function of p.

By solving Poisson equation in cylindrical coordinates, one can find the distribution of electrostatic potential $\Delta\phi(r)$ and carrier density change $\Delta p(r)$ inside NW for a given surface potential change $\Delta\phi_{Si}$ induced by binding of biomolecules, (Supporting Information). Our calculation shows that once the Debye screening length of silicon (without losing generality to other materials), $\lambda_{Si}(=\sqrt{\varepsilon_{Si}k_BT/pe^2})$, becomes 2-3 times longer than R, $\Delta\phi(r)$ remains constant ($\sim \Delta\phi_{Si}$) throughout the radial direction and the whole cross-section of NW is gated by surface charges (Fig.S1 of Supporting Information). Recall that hole (majority carrier) density depends on the Fermi energy E_F as $p = p_i \times \exp[(E_i - E_F)/k_BT]$, (where p_i and E_i are the hole density and Fermi energy for intrinsic semiconductor, respectively),[17] thus surface charge gating effect causes almost uniform hole density change, $\Delta p(r) = p \times \exp(-e\Delta\phi_{Si}/k_BT)$, throughout the radial direction of NW with low carrier density and/or small NW radius, (i.e. $\lambda_{Si} \gg R$). Then the conductance change of NW-FET device is:

$$\Delta G = e\mu \int_0^R 2\pi r \Delta p dr = e\mu \times \pi R^2 \times p \times \{\exp(-e\Delta\phi_{Si}/k_BT) - 1\} \quad (1)$$

where μ is the carrier mobility. We note that although ΔG, the conductance change of device, is the direct signal measured in the sensing experiments, it depends on the specific parameters (diameter, mobility, etc) of individual NW's, thus does not reflect the intrinsic sensitivity. Instead, it is more meaningful to characterize the sensitivity by the dimensionless parameter, $\Delta G/G$, which relates to the volume ratio between the part of NW gated by surface charges (represented by ΔG) and the whole body of NW (represented by G). Therefore, $\Delta G/G$ should reach maximum when the surface/volume of nano-sensor is fully utilized, which happens when the sensor is near carrier depletion (i.e. $\lambda_{Si} \gg R$). With the above expression for ΔG and $G = e \times \mu \times p \times \pi R^2$, the highest sensitivity of a NW-FET sensor is:

$$\Delta G/G = \exp(-e\Delta\phi_{Si}/k_BT) - 1 \quad (2)$$

We emphasize that although we derived Eq.2 with NW treated as a three-dimensional (3D) system, it remains valid when the radial confinement makes the system one-dimensional (1D) since it only relies on the thermally activated nature of carriers, which follow the Boltzmann statistics.[17]

We first used the pH sensing experiment as a model system to study the sensitivity of NW-FET sensor in the various conductance regimes. In a typical pH sensing experiment, the silicon oxide (SiO_2) surface of boron-doped p-type SiNWs was modified with 3-aminopropyltriethoxysilane (Supporting Information). The protonation/deprotonation of amino ($-NH_2$) and silanol (Si-OH) groups changes the surface charges and potential of NW when the pH of electrolyte solution is varied.[2] An on-chip gold pad was used as a gate electrode (V_g) to tune the carrier density inside the NW-FET devices through electrolyte (Fig.2a, inset).[18] Typically, our devices can be turned on/off within $V_g = \pm 0.5$ V. Figure 2a shows the G (V_g) curve in semi-log scale for a NW device with $R = 5$ nm in 10 mM phosphate buffer solution (pH = 7). From our analysis of NW conductance on surface potential, we can infer that the $\lambda_{Si} \gg R$ regime is reached in the $G(V_g)$ plot where G depends exponentially on the electrolyte gate voltage V_g, known as the 'subthreshold regime' in semiconductor device physics

terminology.[17] The parameter characterizing the FET performance in the subthreshold regime is the subthreshold slope *S*, which is defined as the change in V_g needed to tune the device conductance *G* by a factor of ten. The efficiency of gate coupling is defined by a parameter α which is the ratio of between the ideal subthreshold swing at room temperature (60 mV/decade) and the measured *S*.[17,18] For the device in Figure 2a, *S* = 180 mV/decade and thus α = 1/3. For the same device we also extract a trans-conductance $g_m = dG/dV_g \sim 700$ nS/V at V_g less than the threshold voltage V_T (~ 0 V for this device), where *G* depends on V_g linearly (known as the 'linear regime' of FET).

Figure 2b shows the conductance versus time data as 10 mM phosphate buffer solutions with pH from 4 to 9 were sequentially delivered onto the NW sensor surface by a micro-fluidic channel (Supporting Information). Three sets of data are shown at $V_g = -0.4$, 0 and 0.2 V, at which the device is in the linear, near threshold and subthreshold regimes, respectively. At higher pH, deprotonation of amino and silanol groups at the modified SiO_2 surface makes the NW surface more negatively charged, inducing a negative surface potential at NW surface and thus enhancing the conductance of a p-type NW.[2] Although the absolute change of conductance (ΔG) versus pH is larger at $V_g = -0.4$ V, a more distinct signal is observed at $V_g = 0.2$ V, where the NW FET is in the subthreshold regime. This feature is more obvious in terms of relative conductance change, $\Delta G/G = [G - G_{(pH=4)}]/G_{(pH=4)}$, as shown in Figure 2c. It can be seen that from pH = 4 to 9, $\Delta G/G$ increases from ~ 50% at $V_g = -0.4$ V to nearly 600% at $V_g = 0.2$ V, more than an order of magnitude enhancement. We further analyzed the response of our NW pH-sensor at different V_g's by plotting $\Delta G/G$ as a function of pH in Figure 2d. Since in experiments we measured the potential at SiO_2 surface instead of the potential at the Si/SiO_2 interface of NW, we analyzed data in terms of $\Delta\phi_{SiO2}$, the surface potential at the SiO_2/electrolyte interface. The $\Delta G/G$ data at $V_g = -0.4$ V were fitted to a linear dependence: $\Delta G/G_{(pH=4)} = g_m \times \Delta\phi_{SiO2}/G_{(pH=4)}$ with $\Delta\phi_{SiO2}$ as the only fitting parameter. Using g_m = 700 nS extracted from the $G(V_g)$ data in electrolyte-gating measurement, we obtained a fitted $\Delta\phi_{SiO2} \approx -30$ mV/pH, where the negative sign means that the SiO_2 surface is more negatively charged at higher pH. Below we analyzed the pH sensing data in subthreshold regime according to our analysis on the NW sensor response in the $\lambda_{Si} \gg R$ regime.[19] Taking into account of the imperfect gate coupling efficiency, we modified Eq.2 to

$$\Delta G/G = \exp(-\alpha\, e\, \Delta\phi_{SiO2}/k_B T) - 1. \quad (3)$$

Fitting the V_g = 0.2 V data in Figure 2d to Eq.3 with the gate coupling efficiency α = 1/3, we calculate $\Delta\phi_{SiO2} \approx -30$ mV/pH, consistent with the value obtained in the linear regime. It is known that the pH sensitivity in terms of surface potential of materials has a theoretical limit of 60 mV/pH (Nernst equation). Depending on the site densities and the dissociation constants of functional groups on the material surface, the measured $\Delta\phi$(pH) can be lower than the ideal 60 mV/pH.[20,21] The obtained $|\Delta\phi_{SiO2}(pH)| = 30$ mV/pH is in good agreement with the previous results on planar ion-sensitive field-effect-transistor (ISFET) using SiO_2 as a sensing material.[21]

An important advantage of nanoscale chem/bio-sensors is their high sensitivity which may lead to an electrical means to study single biomolecule, complementing to the optical methods.[22-24] Existing theories on ISFET and nanowire sensors concern mostly the screening effect of ionic solutions.[14,21] Here we give a quantitative calculation of the detected surface charge for our NW-sensor with cylindrical geometry and show that the subthreshold regime has the lowest charge detection limit for nano-FET sensors. The charge detected for surface potential $\Delta\phi_{SiO2}$ at the SiO_2/electrolyte interface is given by $Q = C \times \Delta\phi_{SiO2}$, where *C* is the capacitance between the surface charge and the NW/electrolyte system. In calculating *C*, there are three

capacitances in the system: the electrolyte double layer (DL) capacitance C_{DL}, the SiO_2 layer capacitance C_{ox}, and the capacitance of charging NW itself, C_{NW}. When there are surface charges at SiO_2 surface, carriers in the NW and counter ions in the electrolyte will come close to the SiO_2 surface to screen out the surface charge. Since the surface charge of SiO_2 equals to the net charge in NW plus the charge in the electrolyte DL, C can be modeled as C_{DL} in parallel with the series capacitance of C_{ox} and C_{NW}:

$$C=(1/C_{ox}+1/C_{NW})^{-1}+C_{DL} \quad (4)$$

Using double cylinder capacitance formula $2\pi\varepsilon_{SiO2}/\ln(1+d/R)$, we obtained $C_{ox} = 1.4 \times 10^{-15}$ F/μm for typical SiNW with native SiO_2 thickness $d \sim 1$ nm and $R = 5$ nm. The capacitance of NW, C_{NW} characterizes how much the chemical potential (or the Fermi energy E_F) of the carriers shifts with respect to the carrier density change: $C_{NW} = e^2 dp/dE_F$. For non-degenerate carriers in NW, we derived $C_{NW} \approx e^2 \times p \times 2\pi R\lambda_{Si}/k_BT$ for $\lambda_{Si} \ll R$, and $C_{NW} \approx e^2 \times p \times \pi R^2/k_BT$ for $\lambda_{Si} \gg R$, (Supporting Information).[25] Note that C_{NW} decreases quickly as the NW is gated from linear to subthreshold regime. For instance, C_{NW} drops from $\sim 3 \times 10^{-15}$ F/μm to $\sim 5 \times 10^{-18}$ F/μm as p decreases from $1 \times 10^{19}/cm^3$ ($\lambda_{Si} \sim 1.5$ nm) to $1 \times 10^{16}/cm^3$ ($\lambda_{Si} \sim 35$ nm). Therefore, Eq.4 reduces to $C \sim C_{ox} + C_{DL}$ in the high p limit and $C \sim C_{DL}$ in the low p limit. By solving the spatial potential distribution inside DL for cylindrical coordinates, the NW-electrolyte DL capacitance is calculated to be $C_{DL} = x\pi\varepsilon K_1(x)/K_0(x)$ (Supporting Information),[26] where $\varepsilon = 80$ is the dielectric constant of water, $x = R/\lambda$ with λ as the Debye-Huckel screening length of the electrolyte, $K_0(x)$ and $K_1(x)$ are the zero and first-order modified Bessel functions of the second kind. For a 10 mM KCl solution, $\lambda \sim 3$ nm and $R = 5$ nm, $C_{DL} \approx 4.7 \times 10^{-15}$ F/μm. For these parameters, we estimated that our 2-μm long NW-sensor can detect $\Delta Q \sim (C_{ox}+C_{DL}) \times 30$ mV/pH = 2300 e/pH in the linear regime, and $\Delta Q \sim C_{DL} \times 30$ mV/pH = 1800 e/pH in the subthreshold regime.

The charge detection limit $\Delta Q_{min} = C \times \Delta\phi_{min}$, of NW sensors can be reduced by lowering C_{NW} and C_{DL} (the minimal detectable surface potential shift $\Delta\phi_{min}$ is controlled by the electro-chemistry at NW surface and specific noise characteristics of NWs). Therefore, one expects to achieve the best charge sensitivity in the subthreshold regime (where $C_{NW} \to 0$) and in electrolyte with small ionic strength I (as $\lambda \propto I^{-1/2}$), (ref.14). In Table 1, we list the ΔQ_{min} for our sensor in Figure 2, where $\Delta\phi_{min}$ is 5 mV and 0.67 mV in the linear and subthreshold regimes, respectively. We also include the corresponding ΔQ_{min} assuming if a low ionic strength $I = 10$ μM is used. Table 1 shows that it is possible to detect charge as few as several *e's* with a NW FET sensor working in the subthreshold regime and low ionic strength electrolyte.

To further demonstrate the advantage of sensing in subthreshold regime, we carried out detection of prostate specific antigen (PSA), a well-known protein marker for prostate cancer.[3,27,28] Figure 3b shows a typical data set of detecting 15 pM PSA by a SiNW FET sensor at different electrolyte gate voltage V_g. This NW FET is in the linear regime at $V_g = 0$ V and in the subthreshold regime at $V_g = 0.45$ V. Since PSA has an isoelectric point ~ 6.8 (ref.27) and is negatively charged at pH = 7.4, the p-type SiNW FET device conductance increases when PSA binds to its monoclonal antibodies pre-functionalized on SiNW FET surface (Supporting Information). The best signal-to-noise ratio of detecting 15 pM PSA was observed at $V_g = 0.45$ V, (Fig.3b). The absolute conductance change ΔG and the relative conductance change ($\Delta G/G$) for the binding/unbinding signal of 15 pM PSA sample are plotted in the upper panel of Figure 3c as a function of V_g. It clearly shows that the percentage change in conductance increases rapidly as the device is gated into the subthreshold regime, despite a decreasing trend of ΔG. Similar to the analysis on pH sensing, using $g_m = 1650$ nS/V extracted from the conductance vs. electrolyte gate voltage data in the linear regime (Fig.3d), we calculated

$\Delta\phi_{SiO2} = \Delta G/G_m \sim -15$ mV for detecting 15 pM PSA. The $\Delta\phi_{SiO2}$ in the subthreshold regime is determined using a similar approach as the pH sensing analysis. With $\alpha = 0.55$ calculated from the subthreshold slope $S = 110$ mV/decade for this FET device and the measured $\Delta G/G \sim 50\%$, we used Eq.3 to calculate $\Delta\phi_{SiO2} \sim -19$ mV. This value is close to the value obtained in the linear regime. Another practically useful parameter in sensing experiment is the signal-to-noise ratio, which also increases drastically in the subthreshold regime, as displayed in the lower panel of Figure 3c. We rationalize that although ΔG shows some decrease in the subthreshold regime, the conductance noise in our NW FET drops more rapidly, giving rise to a better signal-to-noise ratio.[29] In addition, performing sensing with FET devices completely gated off makes both $\Delta G/G$ and signal-to-noise ratio decreasing, as shown by the data point for $V_g = 0.5$ V in Figure 3c. We believe that this is due to that the noise level in this regime is dominated by the extrinsic sources such as the current leakage between the device and electrolyte, rather than the NW conductance fluctuation. We conclude that for protein detection, the sensor performance is also optimized (in terms of the highest $\Delta G/G$ and signal-to-noise ratio) in the subthreshold regime, consistent with our arguments based on screening length effect on sensitivity as well as the pH sensing experiments.

Last, the detection limit of PSA was compared for a same NW FET device in the linear versus subthreshold regime. Real time conductance sensing data are presented in Figure 4a-b to show the detection limit ~ 0.75 pM for a NW sensor with $g_m = 2800$ nS/V in the linear regime. Figure 4c-f show the time dependent conductance measurements for detecting various PSA concentrations (15 pM, 0.75 pM, 37 fM and 1.5 fM) in the subthreshold regime of the same device, which has subthreshold slope $S = 100$ mV/decade. These data show that the detection limit of this NW FET device was improved from ~ 0.75 pM in the linear regime to ~ 1.5 fM in the subthreshold regime. Therefore, detection in the subthreshold regime of NW FET sensor not only has the merit of much improved conductance response and signal-to-noise ratio, but also better detection limit.

In summary, we propose that the most sensitive NW-FET biosensor should utilize the field gating effect of surface charges throughout the whole cross-section of NW which requires a much longer carrier screening length in NW than its radius. We experimentally demonstrate such scenario by operating the NW-FET sensor in the subthreshold regime when the device is gated inside electrolyte. Our analysis shows that NW FET sensor has the highest percentage conductance response in the subthreshold regime. This has been confirmed in both the pH and PSA sensing experiments. The protein detection limit can be improved by ~ 500 times in concentration by operating the sensor in subthreshold regime instead of linear regime. In addition, we give a quantitative model for calculating the detected surface charge for NW-FET sensors and estimate the charge detection limit for realistic SiNW parameters. We show that charge detection limit is the best also in the subthreshold regime. Our results address the influence of fundamental factors on sensitivity of NW FET bio-sensors and may have broad implications on the sensitivity limits of other FET sensors as well.

Supplementary Material

Refer to Web version on PubMed Central for supplementary material.

Acknowledgments

X.G. acknowledges support of this work by CWRU startup fund and ACS Petroleum Research Fund (Grant 48800-DNI10). C.M.L. thanks NIH National Cancer Institute (Grant R21CA133519) for support of this work.

References

1. Patolsky F, Zheng G, Lieber CM. Anal Chem 2006;78:4260. [PubMed: 16856252]

2. Cui Y, Wei Q, Park H, Lieber CM. Science 2001;293:1289. [PubMed: 11509722]
3. Zheng G, Patolsky F, Cui Y, Wang WU, Lieber CM. Nat Biotechnol 2005;23:1294. [PubMed: 16170313]
4. Li C, Curreli M, Lin H, Lei B, Ishikawa FN, Datar R, Cote RJ, Thompson ME, Zhou C. J Am Chem Soc 2005;127:12484. [PubMed: 16144384]
5. Stern E, Klemic JF, Routenberg DA, Wyrembak PN, Turner-Evans DB, Hamilton AD, LaVan DA, Fahmy TM, Reed MA. Nature 2007;445:519. [PubMed: 17268465]
6. Hahm J, Lieber CM. Nano Lett 2004;4:51.
7. Li Z, Chen Y, Li X, Kamins TI, Nauka K, Williams RS. Nano Lett 2004;4:245.
8. Streifer JA, Kim H, Nichols BM, Hamers RJ. Nanotechnology 2005;16:1868.
9. Chen RJ, Bangsaruntip S, Drouvalakis KA, Kam NWS, Shim M, Li Y, Kim W, Utz PJ, Dai H. Proc Natl Acad Sci USA 2003;100:4984. [PubMed: 12697899]
10. Besteman K, Lee JO, Wiertz FGM, Heering HA, Dekker C. Nano Lett 2003;3:727.
11. Heller I, Janssens AM, Mannik J, Minot ED, Lemay SG, Dekker C. Nano Lett 2008;8:591. [PubMed: 18162002]
12. Nam JM, Thaxton CS, Mirkin CA. Science 2003;301:1884. [PubMed: 14512622]
13. Alivisatos P. Nat Biotechnol 2004;22:47. [PubMed: 14704706]
14. (a) Nair PR, Alam MA. Nano Lett 2008;8:1281–1285. [PubMed: 18386914] (b) Nair PR, Alam MA. IEEE Transactions on Electron Devices 2007;54:3400.
15. Stern E, Wagner R, Sigworth FJ, Breaker R, Fahmy TM, Reed MA. Nano Lett 2007;7:3405. [PubMed: 17914853]
16. Patolsky F, Zheng G, Hayden O, Lakadamyali M, Zhuang X, Lieber CM. Proc Natl Acad Sci USA 2004;101:14017. [PubMed: 15365183]
17. Sze, SM. Physics of Semiconductor Devices. 2nd. Wiley Inter-Science; 1981.
18. Rosenblatt S, Yaish Y, Park J, Gore J, Sazonova V, McEuen PL. Nano Lett 2002:2, 869.
19. Cheng Y, Xiong P, Yun CS, Strouse GF, Zheng JP, Yang RS, Wang ZL. Nano Lett 2008;8:4179. [PubMed: 19367840]
20. Janata J. Analyst 1994;119:2275.
21. van Hal REG, Eijkel JCT, Bergveld P. Sensor Actuat B-Chem 1995;24-25:201.
22. Weiss S. Science 1999;283:1676. [PubMed: 10073925]
23. Zhuang X, Bartley LE, Babcock HP, Russell R, Ha T, Herschlag D, Chu S. Science 2000;288:2048. [PubMed: 10856219]
24. Schuler B, Lipman EA, Eaton WA. Nature 2002;419:743. [PubMed: 12384704]
25. These calculations are valid for low density, non-degenerate carriers in NW. When the quantum degeneracy of carriers is important, the capacitance of NW is $C_{NW} \sim e^2 \times D(E_F)$, where $D(E_F)$ is the density of states at Fermi energy E_F.[18]
26. C_{DL} can be approximated as $C_{DL} \approx \frac{\pi \varepsilon}{\ln(\lambda / R)}$ for electrolyte with low ionic strength (e.g. μM's), using the asymptotic behavior of $K_1(x)$ and $K_0(x)$ at $R/\lambda = x \ll 1$: $K_0(x) \sim -\ln(x)$ and $K_1(x) \sim 1/x$ (Zwillinger, D. CRC Standard Mathematical Tables and Formulae. 31st edition, published by Chapman & Hall/CRC (2002)).
27. Ward AM, Catto JWF, Hamdy FC. Ann Clin Biochem 2001;38:633. [PubMed: 11732646]
28. Armbruster DA. Clin Chem 1993;39:181. [PubMed: 7679336]
29. Detailed study shows that the NW FET conductance noise is the dominant noise source in our experiments (except when the device is completely turned off) and the conductance noise is proportional to carrier density in the device and decreases greatly in the subthreshold regime. Another recent study also found that carbon nanotube FETs have the optimal signal-to-noise ratio in the subthreshold regime: Heller I, Mannik J, Lemay SG, Dekker C. Nano Lett 2009;9:377. [PubMed: 19072626]

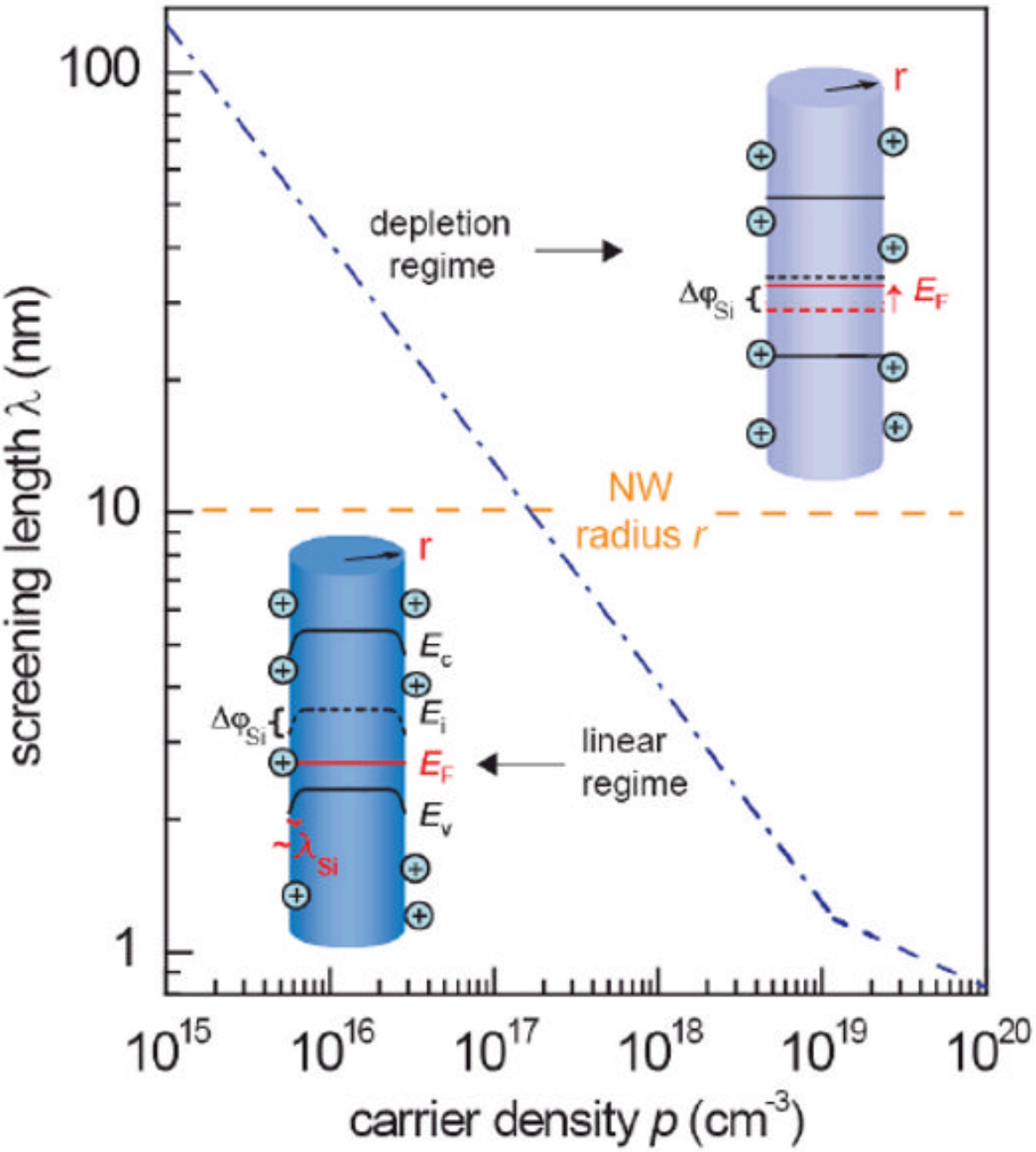

Figure 1.

Screening length effect on the operation and sensitivity of NW FET sensors. The working regime and effectiveness of gating effect induced by molecules at surface of NW-FET sensors are determined by the relative magnitude between carrier screening length λ_{Si} and nanowire size (radius) *R*. In the high carrier concentration regime where $\lambda_{Si} \ll R$, NW-FET works in the linear regime, where the conductance *G* varies with gate voltage linearly. In the low carrier concentration regime where $\lambda_{Si} \gg R$, NW-FET works in the depletion (subthreshold) regime where the *G* varies with gate voltage exponentially. In the linear regime, the field effect of positive/negative surface charges induces band bending and carrier depletion/enhancement

inside the NW within a region of depth ~ λ_{Si}. The amount of band bending at the NW surface is also denoted as surface potential shift $\Delta\phi_{Si}$. In the subthreshold (depletion) regime, carriers in NW have long screening length ($\lambda_{Si} \gg R$) and the field effect of surface charges can gate the whole NW, fully utilizing the high surface volume ratio of NW. In this case, the Fermi level E_F is shifted by $\Delta\phi_{Si}$ relative to the band edges throughout the whole cross-section of NW.

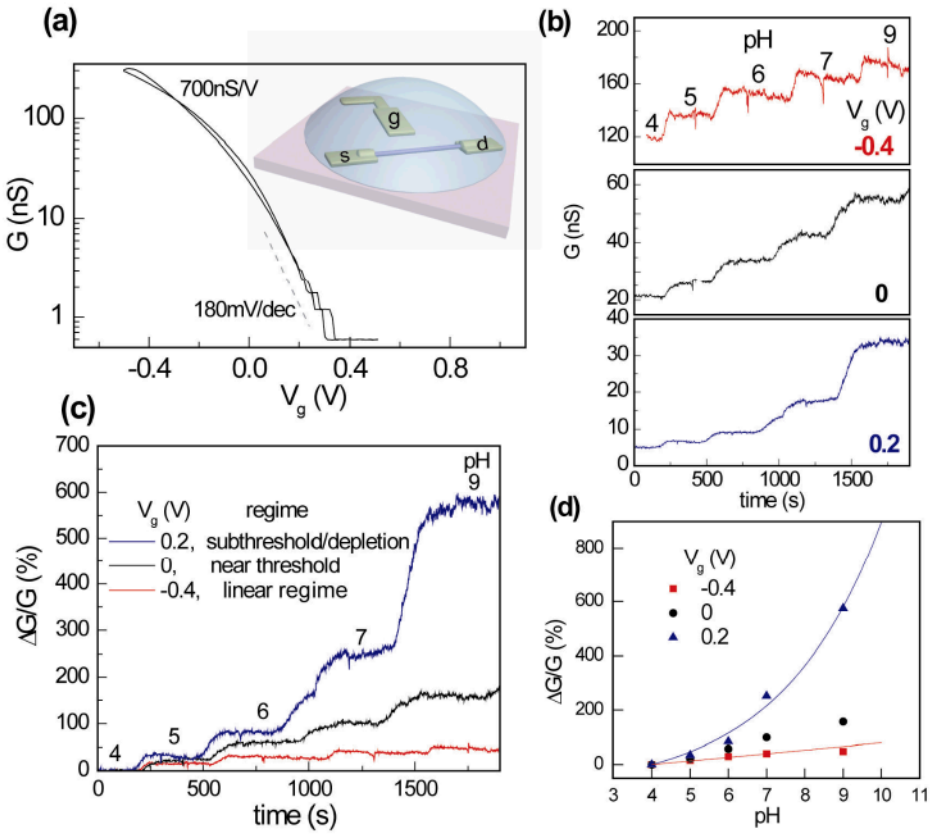

Figure 2.

pH sensing in the linear vs. subthreshold regime of a NW-FET. (a) Conductance *G* vs. electrolyte gate voltage V_g of a p-type silicon NW FET. The inset shows the schematic of electrolyte gating. This device has a trans-conductance ~ 700 nS/V in the linear regime and subthreshold slope *S* ~ 180 mV/decade in the subthreshold regime, with a threshold voltage V_T ~ 0V. (b) Real time conductance data *G*(t) for pH sensing at V_g = −0.4 V (linear regime), 0 V (near threshold voltage) and 0.2 V (subthreshold regime). (c) Real time pH sensing data in (b) plotted as the percentage change, Δ*G*/*G*, with the conductance value at pH = 4 as reference point. In the subthreshold regime (V_g = + 0.2V), the device shows much larger percentage change in conductance as solution pH changes. (d) Device conductance as a function of pH value at V_g = −0.4, 0 and +0.2V. The blue and red lines are exponential and linear responses for pH induced surface potential shift of −30 mV/pH.

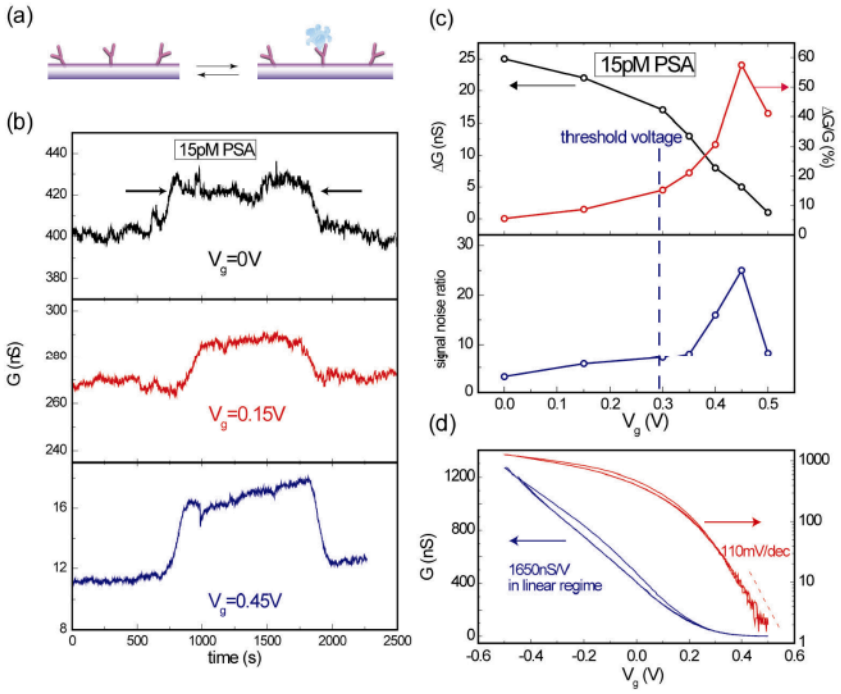

Figure 3.

Sensing PSA/antibody conjugations by NW FET sensor: linear vs. subthreshold regime. (a) Schematic of PSA/PSA-Ab binding/unbinding equilibrium system. PSA-antibody molecules are first linked to nanowire surface. When there are PSA molecules present in sample solution, some antibody sites will be occupied by PSA. The binding of charged PSA molecules induces field gating effect which changes the device conductance. (b) Conductance vs. time data at electrolyte gate voltage V_g = 0, 0.15 and 0.45V when 15 pM PSA sample and buffer solution were sequentially delivered. The increased conductance between arrows was caused by binding of negatively charged PSA molecules on the p-type NW surface. (c) (Top panel) The absolute conductance change ΔG and relative conductance change $\Delta G/G$ vs V_g for sensing of 15 pM PSA. (Bottom panel) signal/noise ratio as a function of V_g for sensing 15pM PSA, which peaks at V_g = 0.45 V in the subthreshold regime before complete depletion of NW. (d) Electrolyte gating performance of this NW device with *G* in linear (left) or log (right) scale.

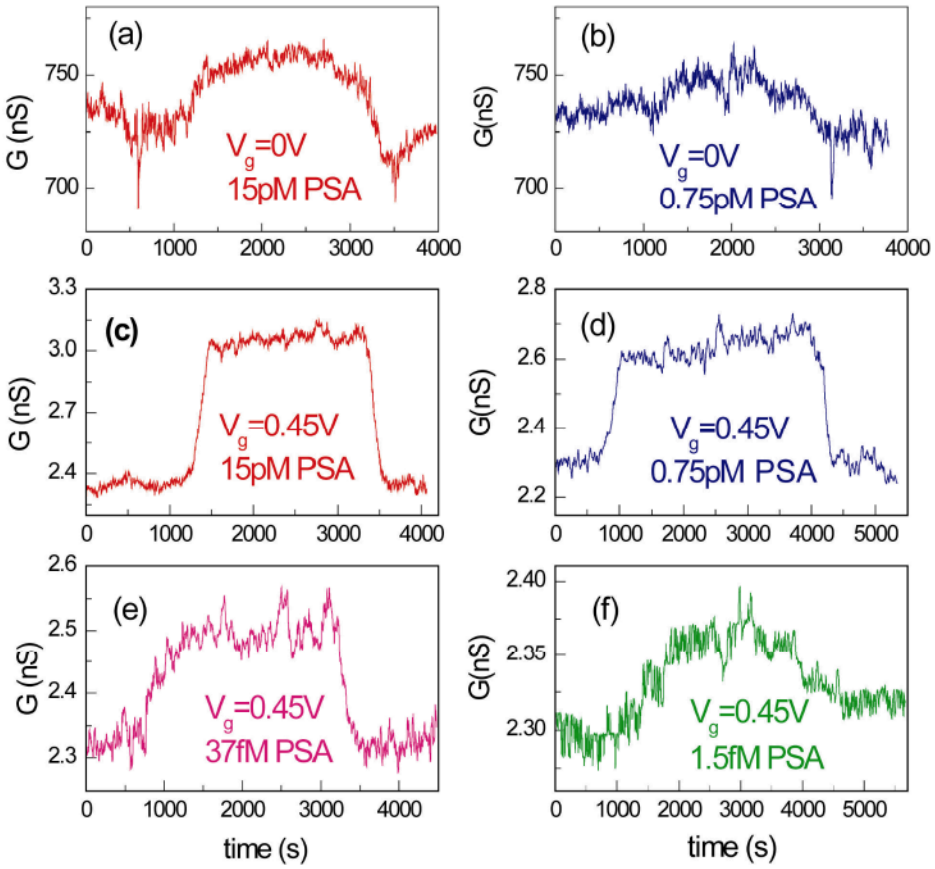

Figure 4.

Greatly Improved PSA detection limit of NW FET sensor in the subthreshold regime (a)-(b) Conductance sensing of 15 pM and 0.75 pM PSA samples by a p-type NW FET sensor at linear regime (V_g = 0 V). The curves show a minimal PSA detection limit ~ 0.75 pM for this device in the linear regime. (c)-(f) Conductance sensing of 15 pM, 0.75 pM, 37 fM and 1.5 fM PSA samples with device in the subthreshold regime (V_g = 0.45 V). It can be clearly seen that the minimal PSA detection limit is improved to ~1.5 fM in the subthreshold regime of this device.

Table 1

Estimated surface charge detection limit $\Delta Q_{min} = C \times \Delta\phi min$ (in units of elementary electron charge, e) per μm-long SiNW FET sensor in 10 mM or 10 μM buffers.

Minimum detectable charges	**Linear regime** $\Delta Q_{min} \sim (C_{ox}+C_{DL}) \times \Delta\phi_{min}$	**Subthreshold regime** $\Delta Q_{min} \sim C_{DL} \times \Delta\phi_{min}$
ΔQ_{min}/μm at I = 10 mM	200 e	20 e
ΔQ_{min}/μm at I = 10 μM	70 e	3 e